DESIGN AND OPTIMIZATION OF A GEOTHERMAL ENERGY STORAGE FEEDING A FULLY RENEWABLE DISTRICT HEATING NETWORK

Natalia Kozlowska[1*], Aitor Cendoya[1], Vincent Lemort[1], Pierre Dewallef[1]

[1] Thermodynamics Laboratory, University of Liège, 4000 Liège, Belgium

*Corresponding Author: natalia.kozlowska@uliege.be

ABSTRACT

The decarbonization of the building sector is of paramount importance to meet EU objectives in terms of greenhouse gas emissions. Many solutions have been documented in the literature ranging from fuel switching towards biomass or electrification using heat pumps. From the point of view of sustainability and air quality, the electrification of building heating is very promising but requires that electricity is generated from renewable resources like solar and/or wind energy. However, the intermittency and seasonality of renewable energy production make it difficult to match the heat demand (i.e., photovoltaic panels produce more during summertime when the heat demand is low, and inversely). The contribution presents the design procedure used to find the best energy generation, storage, and transport of a district heating network supplied by photovoltaic panels and using seasonal geothermal energy storage coupled with short-term battery storage. The optimization problem is solved using a linear programming approach which allows for quick and easy implementation. The rated power and storage capacities are determined together with the optimal operation schedule to target minimum cost and minimum dependency on the electrical grid. The problem of heat losses in geothermal storage receives particular attention as estimated losses are taken into account in the design procedure. Several scenarios considering different ground thermal conductivities and electricity market prices allow for more secure and reliable decision-making at an early stage of the construction process. A fully renewable system without electrical grid connection is not achievable for the considered scenarios due to economic impracticality. The applied test case is also a good example that could be replicated when similar configurations are encountered.

1 INTRODUCTION

The EU faces a pressing need to address the climate and energy security issues associated with space heating, cooling, and domestic hot water supply, which account for 31% of the EU's primary energy demand, actually predominantly sourced from fossil fuels. With 41.3% shares of renewables and climate-neutral heat sources, district heating and cooling networks are a powerful tool to replace fossil-based heating in buildings, currently providing warmth to 67 million EU citizens. Expanding these networks to cover 20% of the EU heat demand by 2030 could save 24 billion cubic meters of gas. The recently proposed 'Fitfor55' package outlines a roadmap for achieving 100% renewable and climate-neutral district heating and cooling networks by 2050, requiring a total investment of 144 billion euros by 2030 [Euroheat and Power, 2023].

The development of renewable energy communities is certainly the most significant evolution in recent years in the way energy systems are designed. It allows multiple individuals to invest in a shared infrastructure for electricity and heat production, a role that was previously exclusive to energy suppliers. The shared infrastructure also consists in a district heating network (DHN) for heat distribution and a electricity distribution network, which are both mainly supplied by a combination of renewable energy sources. However, this new framework requires small-scale energy system design tools that can be used

https://doi.org/10.52202/077185-0168

by small entities with often limited technical and financial resources to implement such projects. It is proposed here to develop an optimization tool for the energy mix of small-scale communities, up to a few dozen buildings. This tool would enable the coupling of two energy vectors (electricity and heat) with some storage methods (batteries and sensible heat storage). The aim is to develop energy systems that are less dependent on fossil resources and that are economically viable. The tool is used as a decision-making technology and a preliminary design tool to provide a rapid overview of the cost, design aspects, and operation schedule of the relevant components with minimal resources and a short time frame.

The presented work involves a feasibility study for a current project, intended to serve as a case study for the developed tool. To align with the rapid progress of the project, a simplification and linearization of the optimization problem have been implemented.

The plateform *Gurobi optimizer* [Gurobi, 2024] is used to solve the optimization problem, through a linear programming (LP) approach. Various techniques are employed for solving linear programming problems, such as the simplex method [Dantzig and Thapa, 2006b] and the interior-point method [Dantzig and Thapa, 2006a]. Gurobi incorporates these methods and dynamically selects the most suitable approach based on the specific characteristics of the given problem.

Various optimization methods for energy systems in the context of the energy transition are discussed in the literature, including mixed-integer nonlinear approaches with multi-objective formulations [Falke et al., 2016], and mixed-integer linear programming models [Omu et al., 2013]. A complete literature review has been conducted by Resimont [Resimont, 2021] on the various optimization methods for energy systems. Finally, a dynamic approach has been implemented in [Cendoya et al., 2024] within the project context, but scenario studies for preliminary decision-making is not feasible due to the extensive computational requirements, consuming considerable time. These optimization formulations are characterized by a high level of complexity, allowing for detailed modeling of the system. However, the complexity of these models can be a barrier to their implementation in the early stages of a project, as they require a significant amount of data and time to be implemented where high accuracy is not yet required. The LP approach is chosen here for its simplicity and rapidity of implementation, which is particularly suitable for the preliminary design of the energy system.

2 PROBLEM STATEMENT

2.1 Context

The developed optimization tool is applied to a test case in Martelange, in the province of Luxembourg of Belgium. A project is currently ongoing in this city to build a new district heating network to supply heat and domestic hot water to a certain number of buildings. The DHN will be supplied by a combination of renewable energy sources, namely photovoltaic panels (PV) and geothermal energy. A slate quarry, one of the cavity of the old mines of the region, is valued as thermal energy storage to store the excess thermal energy produced by renewable sources in low electricity prices periods and sunny days. The available cavity for thermal storage has a volume of 6000 m^3. The DHN is designed to operate between 50°C and 30°C. Additionally, the cold source for the heat pump is an 80000 m^3 reservoir, which operates between 4°C and 12°C. The DHN will be connected to 50 housings, and the thermal demand is estimated to be 387.6 $\text{MWh}_{\text{th}}/\text{year}$ for both heating and domestic hot water demand.

To satisfy the thermal demand, the feasible design includes a heat pump for the base load and electrical resistances for the peak load, with a sensible thermal storage in a cavity of the old mines to store the excess of thermal energy produced. These three components feed the district heating network through primary pumps, which are powered by the electricity produced or imported from the grid. The heat pump extracts energy from another cavity of the old mines, which is used as a cold source. The cold source

https://doi.org/10.52202/077185-0168

needs to be regenerated by a cold user nearby. A schematic of the installation is illustrated in [Cendoya et al., 2024]. An electrical node gathers the production of electricity from photovoltaic panels, the export of surplus solar energy, the import of electricity from the grid, the storage of the excess electricity in batteries, and the connection to the heat pump, the electrical heaters, and the primary pumps. Indeed, the thermal demand is electrified to address dependency issues, leveraging the development of renewable energy sources. The described feasible design is illustrated in the following Figure 1.

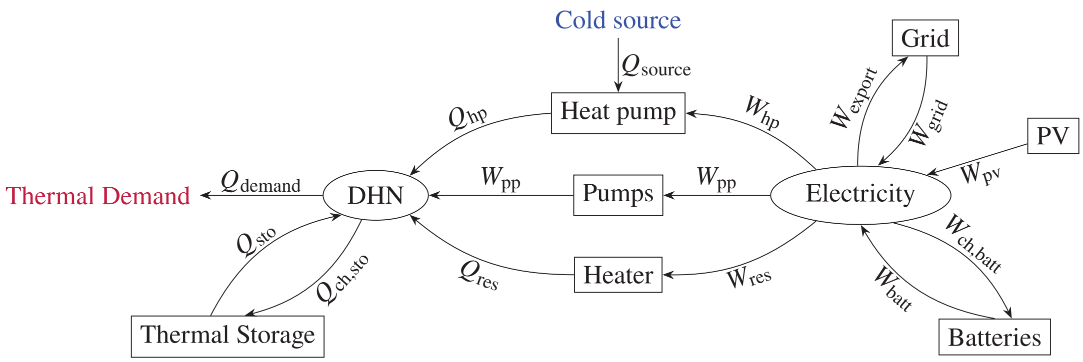

Figure 1: Illustration of the feasible design of the energy mix.

The application of the developed tool allows one to determine the optimal design of the different components of the considered feasible system and their operation behavior to minimize the total system cost.
The decision variables of the problem are the rated powers and capacities of the different components for the appropriate sizing, as well as the instantaneous powers and capacities to determine the optimal operation schedule of the system on an hourly basis over an annual period.

2.2 Objective function

The objective function of the optimization problem aims to minimize the total cost of the system, i.e. the investment cost of the different components and the associated operational cost. The latter is composed of the cost of the electricity bought from the grid, the marginal cost of the different components, the cost associated with the ramp rate of the heat pump, and the fixed costs of the system. By including a cost term for the ramp rate in the objective function, the optimization algorithm can find a solution that balances the trade-off between achieving the desired performance and minimizing the cost associated with rapid changes of the heat pump in the system. The objective function is defined as follows:

$$\begin{aligned} TSC = & \sum_{i,j\in k} \left[\left(c_{0,k}\ \psi_k\right) \left(\dot{Q}_{rated,i} + \dot{W}_{rated,j}\right) + \sum_{t=0}^{8759} \left(\frac{c_{prim,k,t}}{\eta_k} \right) \Delta t \left(\dot{Q}_{i,t} + \dot{W}_{j,t}\right) \right] \\ & + \sum_{l} \left(c_{1,l}\ \psi_l\right) \left(Q_{rated} + W_{rated}\right) + c_{rr,hp} \sum_{t=0}^{8759} \left|RR_{hp,t}\right| + U_{fix,sys}\psi_{sys} \end{aligned} \quad (1)$$

where the indices i and j stand for heating technologies and power generation technologies, respectively. The index l stands for energy storage systems. The annuity factors ψ_k and ψ_l are set for each component,

https://doi.org/10.52202/077185-0168

with an interest rate of 5%. The installation costs $c_{0,k}$ and $c_{1,l}$, as well as the lifetime of the different components, are set as follows in Table 1.

Table 1: Installation costs of the different components.

Power Source	Installation cost	Lifetime
Heat Pump	See Eq.2	20 years
Electrical Heaters	80 €/kW_{th}	20 years
Thermal Storage	80 €/kW_{th}	30 years
Photovoltaic Panels	1000 €/kW_e	20 years
Batteries	600 €/kWh_e	10 years

The cost associated with the installed power of the heat pump is determined by the following equation, derived from actual data provided by the heat pump manufacturer [Viessmann, 2024] :

$$c_{0,hp} = 626 \cdot (\dot{Q}_{rated,hp}/108.7)^{-0.384} \left[\frac{€}{\text{kW}_{\text{th}}}\right] \tag{2}$$

for a range of installed power from 50 kW to 300 kW. The thermal storage system incurs no storage cost related to the installed capacity, given the utilization of an already existing cavity. Nevertheless, a cost associated with the rated power is taken into account due to the nature of geothermal storage, involving expenses for boreholes, casing, and heat exchangers. The cost associated to the ramp rate c_{rr} is 10^{-3} €/kW. The fixed costs of the system $U_{fix,sys}$ for the considered project are estimated to 180,000 €, to which are added 30,000 € of costs for the DHN. The lifetime of the project is set to 25 years. The time step Δt is set to 1 hour.
The index i stands for the two considered energy vectors : heat and electricity. The index j corresponds to the different components of the energy mix.
The energy mix includes renewable sources such as solar energy, which is inexhaustible but intermittent, and geothermal energy, which is renewable in the long term. The only energy incurring a cost is the electricity sourced from the electrical grid. The data used for the price of electricity €/kWh_e corresponds to the year 2023 and is taken from the electricity exchange platform in Belgium (BELPEX) to which are added 65€/kWh_e of connection price [Belpex, 2023]. The levelized total system cost (LTSC) is defined as the total system cost for a year divided by the annual thermal energy demand of the system. The LTSC, which is used to compare the different scenarios, is defined as follows:

$$LTSC = \frac{TSC}{D_{th}} \left[\frac{€}{\text{MWh}_{\text{th}}}\right] \tag{3}$$

2.3 Constraints

The constraints of the problem include various factors that influence the optimal solution. They encompass limitations on the availability of resources, operational constraints, power and energy balances.
In the considered case study, there are two limitations concerning the availability of resources. The photovoltaic rated power is limited to 70 kW_p due to the limited available surface and the available volume of thermal storage in the quarry is limited to 6000 m^3 with a temperature difference of 20°C.
The power balance within the system is expressed through two key equations, the thermal and the electrical power balances. The thermal demand needs to be satisfied at each time step through thermal energy components. The components responsible for heat production, i.e. the heat pump and the resistance, in combination with the thermal storage, are in charge of satisfying the thermal demand. The heat pump

https://doi.org/10.52202/077185-0168

and the resistance are powered by electricity. The thermal demand is electrified to address dependency issues, leveraging the development of renewable energy sources such as photovoltaic panels. The power balance satisfying the thermal demand $\dot{Q}_{demand,t}$ is expressed as :

$$\sum_{i\in\{\text{hp,res,sto}\}} \dot{Q}_{i,t} - \dot{Q}_{\text{charge,sto},t} = \dot{Q}_{\text{demand},t} \qquad \forall t \tag{4}$$

where the thermal demand $\dot{Q}_{demand,t}$ at each time step has been modeled with *Modelica* for the 50 housings in the project context. The detailed description of the model is out of the scope of this work. The thermal demand includes the heating demand, the sanitary water demand, and the losses of the DHN. The geometry of the network is supposed to be fixed, the modeling of the DHN will be the subject of a later work.
The electrical demand is defined by the combined electricity requirements of the heat pump, the resistance, and the primary pumps of the DHN which consumes 3% of the thermal demand. This power is supplied by photovoltaic panels, associated with batteries that store surplus energy and release it when needed, especially during peak hours when electricity costs are higher. The electrical grid compensates for any deficit and allows the export of the surplus energy when needed. The export of energy is characterized as a sink, the sale of energy to the grid is beyond the scope of this work and is thus not considered. The power balance satisfying the electrical requirements is expressed as :

$$\sum_{j\in\{\text{pv,batt,grid}\}} \dot{W}_{j,t} - \dot{W}_{\text{charge,batt},t} - \dot{W}_{\text{export},t} = \sum_{m\in\{\text{hp,res}\}} \dot{W}_{m,t} + \dot{W}_{pp,t} \qquad \forall t \tag{5}$$

The upper bounds of the instantaneous powers $\dot{Q}_{i,t}$ and $\dot{W}_{j,t}$ are limited by their rated powers $\dot{Q}_{rated,i,t}$ and $\dot{W}_{rated,j,t}$ multiplied by τ_{max}. The latter coefficient ranges between 0 and 1. The heat transfer rate is used for illustration :

$$\dot{Q}_{i,t} \leq \tau_{max} \cdot \dot{Q}_{rated,i} \qquad \forall i,t \tag{6}$$

The lower bound follows a similar approach but with τ_{min}, also comprised between 0 and 1.

$$\dot{Q}_{i,t} \geq \tau_{min} \cdot \dot{Q}_{rated,i} \qquad \forall i,t \tag{7}$$

Other instantaneous powers used in this problem need to be bounded, such as the exported electrical power and the charge power for the thermal and electrical storage. The coefficient τ_{max} and τ_{min} are set to 1 and 0 respectively for the instantaneous powers of the different components, except the heat pump minimal power is set to 25% of its rated power.

The thermal storage capacity is determined with the following equation :

$$Q_{rated,sto} = \rho_w \cdot c_{p,w} \cdot V_{sto} \cdot \Delta T_{max} \tag{8}$$

where ρ_w is the density of water, $c_{p,w}$ is the specific heat of water, V_{sto} is the volume of the storage equal to 6000 m^3 and ΔT_{max} is the maximal temperature difference inside the storage. The minimal stored water temperature is 30°C and the maximal temperature is 50°C, the maximal difference ΔT_{max} is then 20°C. Subsequently, the evaluated thermal storage capacity is estimated to 140 MWh_{th}. The heat losses occurring in the storage are modeled in [Cendoya et al., 2024] with a thermal conductivity of the soil, composed of shale, equal to 2.1 W/mK. The model gives a minimal thermal loss of 9 kW_{th} for when water is stored at a temperature of 30°C while thermal losses reach 13 kW_{th} when the water is stored at a higher temperature of 50°C. The specific thermal losses are expressed per unit of storage capacity

https://doi.org/10.52202/077185-0168

available on the site (i.e., 140 $\mathrm{MWh_{th}}$) to obtain the loss coefficients $\tau_{loss,min} = 6.4 \cdot 10^{-5}$ $\mathrm{kW_{th}/kWh_{th}}$ and $\tau_{loss,max} = 9.2 \cdot 10^{-5}$ $\mathrm{kW_{th}/kWh_{th}}$ respectively and to include them in the storage energy balance. The energy balance of the storage system is maintained through an equality constraint at each time step, ensuring the conservation of energy. The thermal storage energy balance considers not only the inflows and outflows of energy to and from the storage but also accounts for the losses within the thermal storage system. As the thermal storage is considered empty when it is filled with water at 30°C, the minimum (i.e., constant) losses are of 9 $\mathrm{kW_{th}}$. As the storage is being filled with hotter water, the corresponding volume is characterised by thermal losses of 13 $\mathrm{kW_{th}}$. The magnitude of the losses in the storage is considered directly proportional to the state of charge of the thermal storage. The energy balance of the thermal storage is expressed as follows:

$$\begin{aligned} \frac{Q_{sto,t} - Q_{sto,t-1}}{dt} &= \dot{Q}_{charge,sto,t} - \dot{Q}_{sto,t} \\ -\tau_{loss,min} \cdot Q_{rated,sto} &- (\tau_{loss,max} - \tau_{loss,min}) \cdot Q_{sto,t} \qquad \forall t \end{aligned} \tag{9}$$

The energy balance of the electrical storage does not include losses within the storage system. However, a round-trip efficiency of 95% is considered for the electrical storage. The energy balance of the batteries is expressed as follows:

$$\frac{W_{batt,t} - W_{batt,t-1}}{dt} = \dot{W}_{charge,batt,t} - \frac{\dot{W}_{batt,t}}{\eta_{batt}} \qquad \forall t \tag{10}$$

The state of charge of the thermal and electrical storage needs to be bounded by the rated capacity of the storage through the following inequalities. The thermal water storage is used for illustration:

$$Q_{sto,t} \leq \phi_{max} \cdot Q_{rated,sto} \qquad \forall t, \ \ \forall i \in \{\text{th,el}\} \tag{11}$$

$$Q_{sto,t} \geq \phi_{min} \cdot Q_{rated,sto} \qquad \forall t, \ \ \forall i \in \{\text{th,el}\} \tag{12}$$

with ϕ_{max} and ϕ_{min} comprised between 0 and 1.
The charging and discharging processes of the battery are subject to specific constraints to ensure the proper functioning of the system. A charge or discharge cycle of the battery is supposed to take at least 3 hours, which is translated into the following constraint :

$$\dot{W}_{charge,batt,t} \cdot 3h \leq W_{rated,batt} \qquad \forall t \tag{13}$$

$$\dot{W}_{batt,t} \cdot 3h \leq W_{rated,batt} \qquad \forall t \tag{14}$$

A ramp rate is considered for the heat pump to control the speed at which the heat pump can adjust its heating output in response to changing demand. The heat pump is used for the base load and is regulated to give a continuous minimal heating output without significant fluctuations. This control is translated into equality constraints, where RR_{max} is set to 1% :

$$\begin{cases} RR^{+}_{hp} & = \dot{Q}_{hp,t} - \dot{Q}_{hp,t-1} \geq 0 \qquad \forall t \\ RR^{-}_{hp} & = \dot{Q}_{hp,t-1} - \dot{Q}_{hp,t} \geq 0 \qquad \forall t \\ \left|RR_{hp}\right| & = RR^{+}_{hp} + RR^{-}_{hp} \leq RR_{\max,i} \dot{Q}_{rated,hp} \frac{60}{\Delta t} \end{cases} \tag{15}$$

The heat pump is assumed to maintain a constant coefficient of performance (COP) of 3.4 during the considered year, a value chosen specifically for the given test case. Additionally, the electric heater is considered to operate with 100% efficiency. These assumptions can be translated into equality constraints as follows:

$$\dot{Q}_{hp,t} = 3.4 \cdot \dot{W}_{hp,t} \qquad \forall t \tag{16}$$

https://doi.org/10.52202/077185-0168

$$\dot{Q}_{res,t} = \dot{W}_{res,t} \qquad \forall t \tag{17}$$

The photovoltaic panels operate at a certain power equivalent to τ_{pv} times their rated power :

$$\dot{W}_{pv,t} = \tau_{pv,t} \cdot \dot{W}_{rated,pv} \qquad \forall t \tag{18}$$

where τ_{pv} corresponds to the efficiency of the photovoltaic panels based on meteorological data and the orientation of the panels, set to an azimuth angle of 0° and a tilt angle of 35°.

2.4 Case studies

The developed tool is applied to the aforementioned test case of the district heating network in Martelange whose purpose is to provide a rapid overview of the cost, design aspects, and operation schedule of the relevant components with minimal resources and a short time frame. The objective function and corresponding constraints of the optimization problem defined in the previous sections are applied to the following scenarios to accomplish this purpose.

The test case is divided into two parts. The first part consists of the application of the developed tool to the reference scenario, which is the scenario where the thermal losses are set to $\tau_{loss,min} = 6.4 \cdot 10^{-5}$ $\mathrm{kW_{th}/kWh_{th}}$ and $\tau_{loss,max} = 9.2 \cdot 10^{-5}$ $\mathrm{kW_{th}/kWh_{th}}$, the electricity market prices are set to the spot market of the year 2023 and the number of housings connected to the DHN is 50. The other parameters are set as described in the previous sections. The objective function is minimized, giving the minimal levelized total system cost (LTSC) of the reference scenario. The optimal design values of the different components resulting from the minimization of the objective function are analyzed together with the optimal operation schedule of the system. The objective behind the application of the developed tool to the reference scenario is to, first, verify the consistency of the tool and, second, to determine if the sizing of the different components aligns with the available resources and the economic viability of the energy system.

The second part of the test case consists of the application of the developed tool to three additional scenarios to assess the impact of some design parameters on the optimal reference design of the system. Those parameters are the thermal losses in thermal energy storage, the electricity market prices, and the number of housings connected to the DHN. For the second scenario, the thermal losses will double to $\tau_{loss,min} = 1.28 \cdot 10^{-4}$ $\mathrm{kW_{th}/kWh_{th}}$ and $\tau_{loss,max} = 1.84 \cdot 10^{-4}$ $\mathrm{kW_{th}/kWh_{th}}$. For the third scenario, the electricity market prices will be set to the year 2022, reflecting significant fluctuations and reaching peak values during certain periods. For the last and fourth scenarios, the number of housings connected to the DHN will be increased to 110, impacting the thermal demand.

3 RESULTS

3.1 Optimal design of the reference scenario

The optimal design values of the different components resulting from the application of the developed tool to the reference scenario are presented in Table 2. The levelized total system cost (LTSC) of the reference scenario is 102.7 €/$\mathrm{MWh_{th}}$. The installed capacity of the thermal storage is 102 $\mathrm{MWh_{th}}$, which is below the limit of 140 $\mathrm{MWh_{th}}$ due to the already existing slate quarries. The installed power of the photovoltaic panels is 59 $\mathrm{kW_p}$, which is also below the imposed limit of 70 $\mathrm{kW_p}$ due to the limited available surface on the site. The high cost of batteries, set at 600 €/$\mathrm{kWh_e}$, excludes them from the optimal energy mix. This implies that from an economic standpoint, having a large number of photovoltaic

https://doi.org/10.52202/077185-0168

panels may not be necessary if surplus electricity cannot be effectively stored. The optimal design values are then consistent with the available resources.

Table 2: Optimal design values for the reference scenario with a LTSC of 102.7€/MWh$_{th}$.

Power Source	**Installed Power/Capacity**
Heat Pump	85 kW$_{th}$
Electrical Heaters	22 kW$_{th}$
Thermal Storage	102 MWh$_{th}$
Photovoltaic Panels	59 kW$_{e}$
Batteries	0 kWh$_{e}$

For reminder, the heat pump is used for the base load and the electrical heater for the peak load. The heat pump is regulated to give a continuous minimal heating output (25% of nominal heating capacity) without significant fluctuations. The peak power of the thermal demand occurs in the middle of December for a peak value of 543 kW$_{th}$, which asserts the good use of the thermal energy storage as the capacity of the heat pump together with the electrical heater is 107 kW$_{th}$. The size of the heat pump does not need to be significant to satisfy the thermal demand. The behavior of the heat pump is illustrated in Figure 2 with a load duration curve of its produced heating capacity. The heat pump operates at its rated capacity for slightly less than 50% of the time.

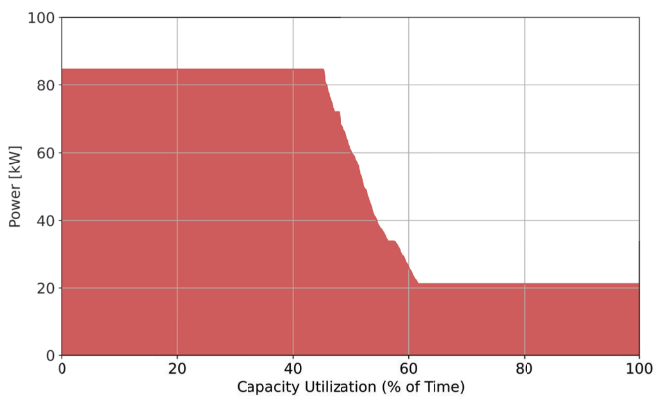

Figure 2: Heat pump heating output: Annual load duration curve.

The reference scenario is illustrated in Figure 3 in the form of a Sankey diagram, a graphical representation used to visualize energy flows in the form of arrows, with the width of the arrows proportional to the quantity of energy they represent. This graphical representation allows for a clear and concise overview of the energy flows within the system during a year. The thermal demand is divided among the load required for buildings, sanitary hot water, and losses from the district heating network, which are considered constant since it is not modeled, as it is beyond the scope of this study. The photovoltaic panels are optimally sized with a self-consumption rate of 99.2%, given the minimal surplus of electricity exported. The self-sufficiency rate is 38.7%. It shows that a significant amount of electrical energy needs to be imported from the grid to satisfy the electrical demand, including the heat pump, the electrical heaters, and the primary pumps. Despite the lack of batteries, the energy mix leverages photovoltaic production and takes advantage of low-price electricity periods to power thermal storage, the cost of

https://doi.org/10.52202/077185-0168

which is minimized through the valorization of slate quarries. The regeneration of the cold source by a nearby cooling load is necessary. Although not depicted in the current diagram due to the absence of immediate cooling demand in the project context, it is crucial to account for the soil's capacity to regenerate heat.
The fact that the optimal design is not self-sufficient implies that it is not fully renewable. However, the electricity imported from the grid to meet the energy requirements comes at a low cost, a factor reflected in the optimal LTSC. Consequently, the composition of the electricity mix during periods of low prices is frequently dominated by renewable sources, such as solar energy on sunny days. Thus, it can be asserted that the imported electricity from the grid is not exclusively derived from fossil fuels, contingent on the prevailing electricity mix in Belgium at the time of import [Agency, 2024].

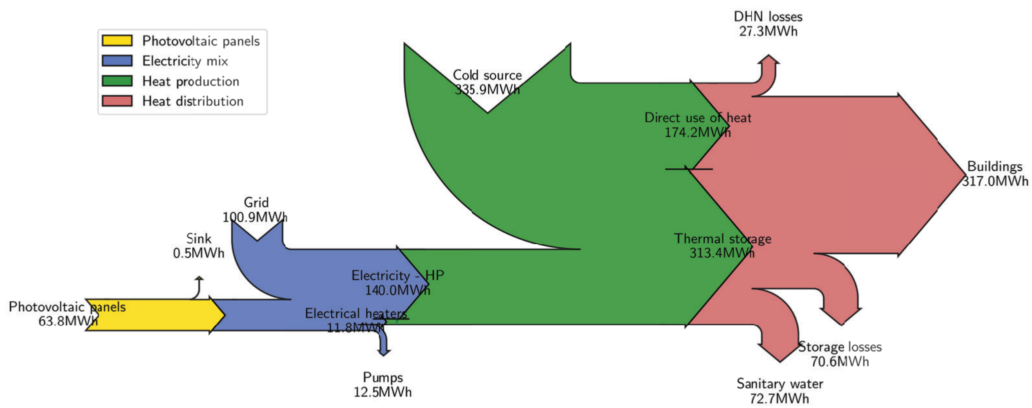

Figure 3: Sankey diagram of the reference scenario.

The use of the developed tool for the reference scenario allows for results in a time frame of around five minutes, which is a significant advantage for a preliminary design with minimal information. Also, it allows one to estimate the sufficiency of available resources, the approximative needed size of the different components, and the economic viability of the energy system, which is very useful for the early stages of the construction process.

3.2 Impact of the variation of parameters on the optimal reference design of the system

The impact of the variation of parameters on the reference optimal design of the system is assessed through the application of the tool to three additional scenarios, where a parameter is varied in each scenario. The goal of this section is to analyze how the optimal reference design varies and how the levelized total system cost is impacted by the variation of these parameters. The thermal storage losses are doubled in the second scenario, the number of housings connected to the DHN is increased to 110 in the third scenario and the electricity market prices are set to the year 2022 in the last scenario. As a reminder, the electricity market prices in the reference scenario are set to those of the year 2023, considered a typical year. This is in contrast to 2022, which experienced an energy crisis, leading to significant fluctuations and peaks. All the scenarios are summarized in Table 3.

As long as 50 housings are connected to the DHN, there is no need for the installed power of the heat pump to exceed 90 kW_{th}. The optimal design value of the heat pump is not much impacted by the variation of the thermal losses in the thermal storage and the electricity market prices. Therefore, the

https://doi.org/10.52202/077185-0168

Table 3: Optimal design values and LTSC for the four scenarios.

Scenarios	1 Reference	2 Storage losses x2	3 110 housings	4 Grid prices 2022
Heat pump [kW_{th}]	85	87	193	88
Electrical heater [kW_{th}]	22	10	1	22
Thermal storage [MWh_{th}]	102	63	137	102
Photovoltaic panels [kW_e]	59	43	70	70
Batteries [kWh_e]	0	0	0	36
LTSC (€/MWh_{th})	102.7	108.3	79.2	123.2

decision not to invest in a heat pump exceeding 100 kW_{th} is consistent. However, if more housings are connected to the DHN, the optimal design value of the heat pump will increase accordingly.
The electrical resistances have an installed power that varies depending on the thermal storage capacity to meet fluctuating heat demand. They play an essential role in the system, achieving the desired performance with instantaneous power changes, and are used to handle peak loads. Having a few dozen kilowatts installed for the electrical heaters should be sufficient to cover peak loads and provide a backup solution in case of scenario changes.
The installed capacity of the thermal energy storage never exceeds its limit of 140 MWh_{th} in any of the scenarios. The available resources are then sufficient to optimally satisfy the thermal demand, even with the variation of the concerned parameters.

The upper limit of 70 kW_p for the photovoltaic panels becomes an active constraint when electricity market prices are set to the year 2022 as it underwent significant fluctuations and reached peak values during certain periods, making the photovoltaic panels more profitable. The limit of 70 kW_p is also reached when 110 housings are connected to the DHN.
The batteries are not included in the optimal energy mix in any of the scenarios, except in the third scenario where the electricity market prices are set to the year 2022. Indeed, as for the photovoltaic panels, the batteries become more profitable when the electricity market prices reach high peak values.

The self-sufficiency rates for scenarios 2, 3, and 4 are 28.5%, 22.6%, and 45.5%, respectively. These rates decrease with the rise in storage losses and the number of residences connected to the DHN. This decrease is consistent, given the limitations on the installed power of photovoltaic panels and the increased electrical demand. The notable self-sufficiency rate in scenario 4 is attributed to the inclusion of batteries. These batteries store excess energy and release it when needed, particularly during peak hours when electricity costs are higher. None of the scenarios achieve a fully renewable system due to economic impracticality.

The costs associated to the scenarios where 50 housings are considered (i.e. 1, 2 and 4) have a value of respectively 102.7, 108.3 and 123.2 €/MWh_{th}. The scenario 1 is the reference scenario where the thermal storage losses are set to their modeled value and the electricity market prices are set to the year 2023 which experienced a stable market. The increase of cost in the two latter scenarios results from the variation of impactful parameters to a worst scenario case. The scenario 3 experiences a low LTSC of 79.2 €/MWh_{th}, which is due to several reasons. The fixed costs of the system infrastructure and the DHN are distributed across a greater number of residences, resulting in a reduced per-unit energy cost. Additionally, the per-unit investment cost for production of energy services, such as those provided by heat pumps, decreases with larger systems. Such systems frequently improve energy production and

 https://doi.org/10.52202/077185-0168

distribution efficiency, possibly due to better resource utilization or infrastructure optimization. The thermal storage, which incurs a minor cost, also helps to reduce the need for peak power production.

The ability to vary the most significant parameters and studying worst-case scenarios helps the designer to set an upper limit on the total cost, ensuring it never exceeds a certain threshold value. The quick and simplified design allows for preliminary decision-making in an early stage of a project. Additionally, it helps determining the significance of the parameter variations and their impact on the final outcome compared to the reference scenario. This provides more precise estimates for subsequent work requiring detailed models.

4 CONCLUSION

The present contribution is intended to propose a methodology for the rapid optimal design of an energy system encompassing a large range of technical solutions for the conversion and the storage of energy. The optimization problem approach is explicitly stated and can be reproduced by using available optimization tools.

The optimal design values of the different components resulting from the application of the tool to the reference scenario are consistent with the available resources, i.e. 400 m^2 of available surface for the installation of photovoltaic panels and 6000 m^3 of available volume for the thermal storage. An optimal sizing of the different components and their annual energy flows are obtained in a time frame of around five minutes, subject to the computational capacity of the computer. Such an application framework is extremely useful in a pre-study stage to determine the outline of the optimal energy system.

Furthermore, the tool evaluates the impact of design parameters on the optimal solution, like the electricity prices or the storage losses, allowing for the study of worst-case scenarios and establishing upper limits on installed power, capacity, and total cost.

A fully renewable system is not achieved due to economic impracticality. With the available resources, the importation of electricity from the grid is deemed essential to meet energy requirements at an appropriate cost.

The tool capability provides more accurate estimates for subsequent work requiring detailed models. Consequently, the tool proves to be a valuable asset in the early phases of the construction process, as for the ongoing project in Martelange, offering a quick and simplified design for preliminary decision-making.

The presented tool still requires some improvements, such as the modeling and the coupling of the district heating network to accurately account for thermal pipe losses. In this work, these losses are assumed to be constant due to fixed pipe geometry. Electrical and thermal nodes are accounted for, but the interconnecting flows between them are not considered. Additionally, the tool could benefit from incorporating the sale of electrical energy to the grid, a factor not considered in this work. Certain simplifications have been made, including the constant coefficient of performance of the heat pump. The drawback of linear programming lies in the need to linearize non-linear cost functions, such as those related to unit installation power or capacity, for instance. Nevertheless, the tool's primary aim is to offer a rapid overview of optimal design aspects within a few minutes timeframe, and it is not intended to provide a detailed overview of the system, as that would require more resources and a longer timeframe.

NOMENCLATURE

https://doi.org/10.52202/077185-0168

Abbreviations

DHN	District Heating Network
PV	Photovoltaic panels
$LTSC$	Levelized Total System Cost
COP	Coefficient of Performance

Symbols

$\dot{Q}$	Heat transfer rate (W)
$\dot{W}$	Power (W)
Q	Thermal energy (J)
W	Electrical energy (J)
c	Cost (€)
η	Efficiency (−)
ψ	Annuity factor (−)
V	Volume (m^3)
ρ	Density (kg/m^3)

Subscripts and superscripts

th	thermal
el	electrical
hp	heat pump
sto	storage
$batt$	batteries
t	time
rr	ramp rate
res	electrical heater
pv	photovoltaic panels

REFERENCES

[Agency, 2024] Agency, I. E. (2024). World energy statistics and balances. Last accessed 17 February 2024.

[Belpex, 2023] Belpex (2023). Elexys : Spot belpex 2023. Last accessed 12 Januray 2024.

[Cendoya et al., 2024] Cendoya, A., Ransy, F., Lemort, V., Kozlowska, N., and Dewallef, P. (2024). Modelling and simulation of a seasonal undergournd water storage coupled with photovoltaic panels, heat pump and district heating network for providing local renewable heating to a residential district. In *Proceedings of ECOS 2024*, Rhodes Greece.

[Dantzig and Thapa, 2006a] Dantzig, G. B. and Thapa, M. N. (2006a). *Linear Programming: Interior-Point Methods*, pages 392–420. Springer New York, New York, NY.

[Dantzig and Thapa, 2006b] Dantzig, G. B. and Thapa, N. M. (2006b). *Linear Programming: The Simplex Method*, pages 355–391. Springer New York, New York, NY.

[Euroheat and Power, 2023] Euroheat and Power (2023). Unleashing the potential of efficient district heating and cooling to decarbonise europe. Technical report.

[Falke et al., 2016] Falke, T., Krengel, S., Meinerzhagen, A.-K., and Schnettler, A. (2016). Multi-objective optimization and simulation model for the design of distributed energy systems. *Applied Energy*, 184:1508–1516.

[Gurobi, 2024] Gurobi (2024). Gurobi optimizer reference manual.

[Omu et al., 2013] Omu, A., Choudhary, R., and Boies, A. (2013). Distributed energy resource system optimisation using mixed integer linear programming. *Energy Policy*, 61:249–266.

[Resimont, 2021] Resimont, T. (22 December 2021). *Strategic outline and sizing of district heating networks using a geographic information system*. PhD thesis, ULiège - Université de Liège, Liège, Belgium. `https://hdl.handle.net/2268/262651`.

[Viessmann, 2024] Viessmann (2024). Viessmann technical documentation. Last accessed 11 Januray 2024.

https://doi.org/10.52202/077185-0168